Molecular Gradients

DOI: 10.1002/anie.200705824

Formation of Molecular Gradients on Bipolar Electrodes**

*Christian Ulrich, Olof Andersson, Leif Nyholm, and Fredrik Björefors**

Surfaces with gradients in their chemical properties or molecular functionalities are highly attractive because of their potential sensor and biomimetic applications. Surface-tension effects[1,2] and protein adsorption[3,4] can also be studied by using molecular gradients. Several gradient-forming approaches have been demonstrated to date; these approaches are based, for example, on diffusion,[5] electric fields,[6] microfluidic systems,[7] and immersion procedures.[8] Bohn and co-workers proposed an electrochemical method to form gradients on very thin metal substrates (of about 50 nm) by using in-plane electrochemical potentials.[9] In that method, a potential gradient was generated across the surface using a bipotentiostat. Monolayer gradients of alkane thiols with varying widths and positions could thus be created on the surface.

Herein, we propose the use of a bipolar electrode as a means to establish a potential gradient across a surface. A voltage (or current) source and two electrodes are used to induce an electric field in a solution containing a conducting surface (see Figure 1). The surface can then become a bipolar electrode, that is, an electrode that acts as both anode and cathode. This occurs when the electric field parallel to the surface exceeds a certain threshold value, thereby inducing redox reactions at both ends. Thus, in the present approach, a potential gradient is induced across an electrode by creating an electric field in the solution and not by controlling the potential of the electrode. Duval et al.[10] modeled the electrochemical behavior of planar bipolar electrodes in a lateral electric field in conjunction with electrokinetic experiments. Bipolar electrodes have further been used in industrial applications[11] as well as in poorly conducting media[12] or for electrochemiluminescence-detection purposes.[13]

The potential difference between a point on the bipolar electrode and the solution varies laterally along the surface, and the driving force for electrochemical reactions varies accordingly. The rate of the redox reactions is highest at the edges of the electrode and decreases towards the center of the surface. This behavior can be used to create a surface gradient of molecular functionality, because the adsorption or desorption of a specific molecule can be controlled through the bipolar-electrode reactions. However, to our knowledge, these properties have not been exploited until now to generate molecular gradients. The major advantage of this technique is that the electrode can be of virtually any thickness, shape, and material (as long as it is conductive). Furthermore, the method is fast and based on a simple experimental setup and the surface itself does not have to be electrically contacted.

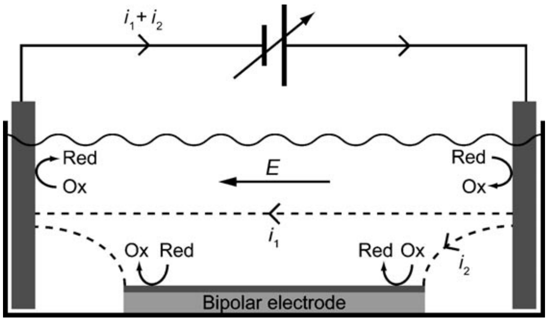

Figure 1. Experimental setup showing the current paths arising from electrochemical reactions taking place on the bipolar electrode. The bipolar electrode typically consists of a metal layer deposited on an insulating substrate. A variable voltage source is used to control the total current between two electrodes (for example, two stainless-steel electrodes).

Imaging surface plasmon resonance[14] (iSPR) was used to display the cathodic and anodic regions of the bipolar electrode and thus characterize the electric-field-induced potential gradients. A setup similar to that shown in Figure 1 was placed on top of a prism in an iSPR instrument. The cell consisted of a polytetrafluoroethylene (PTFE) body pressed against a gold surface with an O-ring in between. If the electrochemical reactions give rise to any changes in the refractive index close to the surface, the SPR response will change accordingly. In the experiments, a current was passed through a solution of $K_4[Fe(CN)_6]$ (200 mM) using two stainless-steel electrodes. The oxidation of the species could be monitored at different locations on the surface because of the difference in the refractive indices of $[Fe(CN)_6]^{3-}$ and $[Fe(CN)_6]^{4-}$. Figure 2 depicts the changes in the SPR response of the anodic part of the bipolar electrode for different total currents. To ensure that only the reactions of interest were being monitored, we evaluated the intensity differences between the images taken five seconds after the current was switched on and those obtained at open circuit. The main cathodic reaction at the other end of the surface was the reduction of water. Upon increasing the current, the width of the gradient decreases and the gradient region shifts towards the center of the surface. This behavior is the result of a larger

---

[*] C. Ulrich, O. Andersson, Prof. F. Björefors
Division of Applied Physics
Department of Physics, Chemistry and Biology (IFM)
Linköping University, 58183 Linköping (Sweden)
Fax: (+46) 13-288-969
E-mail: frebj@ifm.liu.se
Homepage: http://people.ifm.liu.se/frebj/
Prof. L. Nyholm
Department of Materials Chemistry
Uppsala University, P.O. Box 538, 75121 Uppsala (Sweden)

[**] This work was supported by VINNOVA, SSF, and CTS. The authors thank Hans Sundgren and Ingemar Lundström for valuable discussions.

Supporting information for this article is available on the WWW under http://www.angewandte.org or from the author.

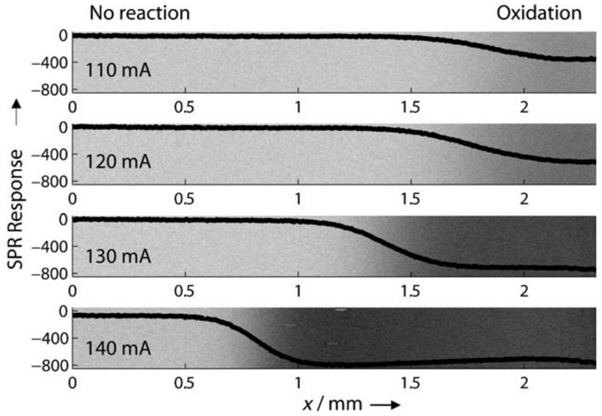

Figure 2. Changes in the SPR response owing to the change in the refractive index when $[Fe(CN)_6]^{4-}$ is oxidized to $[Fe(CN)_6]^{3-}$ (at different total currents). The lines show the mean intensity change in the SPR images.

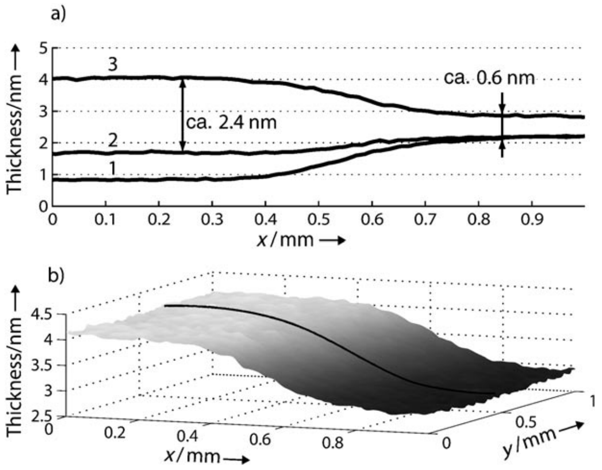

Figure 3. a) Line profiles, obtained from imaging-null-ellipsometry measurements, in which the thicknesses of the gradients observed after the different preparation steps are shown. Line 1 exhibits the result of the desorption of mPEG, line 2 shows that obtained after backfilling with aPEG, and line 3 represents the resulting protein gradient. b) Thickness map of the protein gradient (the line shows the region from which the line profile was taken).

iR drop in the electrolyte, and it clearly demonstrates the possibility to control the position and the width of the gradient region. The sigmoidal curves shown in Figure 2 results from the logarithmic relationship between the potential difference and the concentration ratio of $[Fe(CN)_6]^{3-}$ and $[Fe(CN)_6]^{4-}$. The small response increase observed for a distance of about 2 mm (at a current of 140 mA) can be attributed to the geometry of the iSPR cell close to the O-ring, which influences the mass transport of the redox species.

Different gradients (for various applications) can be formed using this method; for example, we prepared gradients of both copper and electropolymerized polypyrrole on gold. As a demonstration of the possibility to straightforwardly design and modify surfaces containing gradients in their chemical properties—and attach biorelevant molecules to such surfaces—we used self-assembled monolayers (SAMs) and protein-immobilization procedures. SAMs offer an easy way to form molecular gradients on surfaces, because thiols can be electrochemically desorbed both cathodically and anodically. A gold surface covered with a SAM of $HS{-}C_2H_4{-}(O{-}C_2H_4)_6{-}OCH_3$ (mPEG) was employed as the bipolar electrode (Figure 1). A current of 15 mA was then passed through the electrolyte (1 M KOH in ethanol) for 30 s to remove the thiol species from the cathodic part of the bipolar gold electrode. Imaging null ellipsometry was then used to measure the thickness of the SAM on the cathodic side. As can be seen in Figure 3 a (line 1), a molecular-gradient region with a width of about 0.5 mm was formed. A similar gradient was also observed on the anodic side but because of the possible formation of gold oxide, this gradient was not further evaluated. Figure 3 a also suggests that the surface in the electrochemically desorbed region was not perfectly clean, which can be deduced from the thickness indicated by line 1 (which is of about 0.8 nm). We ascribe this result to the contamination of the bare gold surface with hydrocarbon species present in the surrounding air during the ellipsometric analysis. The same effect was also observed after the reduction of a SAM on a gold working electrode in a standard three-electrode setup. However, this is a minor problem because the contaminants can be displaced by immersing the surface in a backfilling solution containing a second thiol species. To provide binding sites for the protein, the surface was backfilled for 60 s with $HS{-}C_2H_4{-}(O{-}C_2H_4)_8{-}COOH$ (aPEG). The gradient after the backfilling step can be seen in Figure 3 a (line 2). A longer incubation time results in a full aPEG monolayer, but it may also give a higher degree of substitution of the mPEG species. The carboxy groups were then activated for 20 min and used as binding sites when the surface was incubated in lysozyme (30 min). The thickness of the resulting lysozyme layer on the activated aPEG was around 2.4 nm, which almost corresponds to a full monolayer of the protein.[15] The lysozyme film on the mPEG part of the surface had a thickness of about 0.6 nm, which is possibly the result of an unspecific physisorption of the protein and/or the substitution of some mPEG molecules with aPEG species during the backfilling step. A section of the thickness map obtained on the protein surface is shown in Figure 3 b, where—as expected—no thickness variations are observed on the surface parallel to the protein gradient.

In conclusion, the method described herein is suitable for the generation of functional molecular gradients on conducting surfaces. It is a fast and straightforward technique that does not require access to advanced laboratory equipment. Moreover, a wide variety of setup geometries and electrolytes can be used, thus making it a very versatile approach. One way to widen the gradient region would be to place the bipolar surface at a given angle with respect to the other two electrodes, an approach that is currently being studied. Moreover, it is possible to produce a semispherical electric field in the solution by replacing one of the two electrodes with a wire and placing it above the bipolar electrode. This setup would generate a reaction region in the middle of the surface, with gradients on both sides of the wire. Future studies on the composition, the degree of phase separation, and the organization of the thiol gradients will be performed by using electron spectroscopy for chemical analysis (ESCA), scanning probe techniques, and FT-IR microscopy.

Experimental Section

For experimental details about the iSPR and ellipsometric measurements, see the Supporting Information.

The carboxy groups were activated using a mixture of 1-ethyl-3-(3-dimethylaminopropyl)carbodiimide (EDC, 0.2 mM) and *N*-hydroxysuccinimide (NHS, 0.05 mM). The result was a reactive succinimide ester which was able to form covalent bonds with the amine groups in the protein. Lysozyme was dissolved in Bis-Tris buffer (30 mM, pH 7.0) to a concentration of 1 mg mL^{-1}.

Received: December 19, 2007

Keywords: bipolar electrodes · electrochemistry · imaging · molecular gradients · surface chemistry

---

[1] M. K. Chaudhury, G. M. Whitesides, *Science* **1992**, *256*, 1539–1541.

[2] B. S. Gallardo, V. K. Gupta, F. D. Eagerton, L. I. Jong, V. S. Craig, R. R. Shah, N. L. Abbott, *Science* **1999**, *283*, 57–60.

[3] M. Mrksich, J. R. Grunwell, G. M. Whitesides, *J. Am. Chem. Soc.* **1995**, *117*, 12009–12010.

[4] C. D. Tidwell, S. I. Ertel, B. D. Ratner, B. J. Tarasevich, S. Arte, D. L. Allara, *Langmuir* **1997**, *13*, 3404–3413.

[5] a) B. Liedberg, P. Tengvall, *Langmuir* **1995**, *11*, 3821–3827; b) M. Riepl, M. Östblom, I. Lundström, S. C. T. Svensson, A. W. Deiner van der Gon, M. Schäferling, B. Liedberg, *Langmuir* **2005**, *21*, 1042–1050.

[6] a) K. Y. C. Lee, J. F. Klingler, H. M. McConnell, *Science* **1994**, *263*, 655–658; b) J. T. Groves, S. G. Boxer, H. M. McConnell, *Proc. Natl. Acad. Sci. USA* **1998**, *95*, 935–938.

[7] N. L. Jeon, S. K. W. Dertinger, D. T. Chiu, I. S. Choi, A. D. Stroock, G. M. Whitesides, *Langmuir* **2000**, *16*, 8311–8316.

[8] S. Morgenthaler, S. Lee, S. Zucher, N. D. Spencer, *Langmuir* **2003**, *19*, 10459–10462.

[9] a) R. H. Terrill, K. M. Balss, Y. Zhang, P. W. Bohn, *J. Am. Chem. Soc.* **2000**, *122*, 988–989; b) K. M. Balss, B. D. Coleman, C. H. Lansford, R. T. Haasch, P. W. Bohn, *J. Phys. Chem. B* **2001**, *105*, 8970–8978; c) S. T. Plummer, P. W. Bohn, *Langmuir* **2002**, *18*, 4142–4149; d) S. T. Plummer, Q. Wang, P. W. Bohn, R. Stockton, M. A. Schwartz, *Langmuir* **2003**, *19*, 7528–7536.

[10] a) J. Duval, J. M. Kleijn, H. P. van Leeuwen, *J. Electroanal. Chem.* **2001**, *505*, 1–11; b) J. F. L. Duval, H. P. Leeuwen, J. Cecilia, J. Galceran, *J. Phys. Chem. B* **2003**, *107*, 6782–6800; c) J. F. L. Duval, J. Buffle, H. P. van Leeuwen, *J. Phys. Chem. B* **2006**, *110*, 6081–6094.

[11] F. C. Walsh, *Pure Appl. Chem.* **2001**, *73*, 1819–1837.

[12] M. Fleischmann, J. Ghoroghchian, D. Rolison, S. Pons, *J. Phys. Chem.* **1986**, *90*, 6392–6400.

[13] W. Zhan, J. Alvarez, R. M. Crooks, *J. Am. Chem. Soc.* **2002**, *124*, 13265–13270.

[14] B. Rothenhäusler, W. Knoll, *Nature* **1988**, *332*, 615–617.

[15] F. Leisten, M. Weichmann, O. Enders, H.-A. Kolb, *J. Colloid Interface Sci.* **2006**, *298*, 508–514.